Environmental Science & Technology

ARTICLE

pubs.acs.org/est

Quantifying Differences in the Impact of Variable Chemistry on Equilibrium Uranium(VI) Adsorption Properties of Aquifer Sediments

Deborah L. Stoliker,[†,*] Douglas B. Kent,[†] and John M. Zachara[‡]

[†]U.S. Geological Survey, 345 Middlefield Rd. MS 496, Menlo Park, California 94025, United States

[‡]Pacific Northwest National Laboratory, Richland, Washington, United States

Supporting Information

ABSTRACT: Uranium adsorption−desorption on sediment samples collected from the Hanford 300-Area, Richland, WA varied extensively over a range of field-relevant chemical conditions, complicating assessment of possible differences in equilibrium adsorption properties. Adsorption equilibrium was achieved in 500−1000 h although dissolved uranium concentrations increased over thousands of hours owing to changes in aqueous chemical composition driven by sediment-water reactions. A nonelectrostatic surface complexation reaction, >SOH + UO_2^{2+} + $2CO_3^{2-}$ = >$SOUO_2(CO_3HCO_3)^{2-}$, provided the best fit to experimental data for each sediment sample resulting in a range of conditional equilibrium constants (logK^c) from 21.49 to 21.76. Potential differences in uranium adsorption properties could be assessed in plots based on the generalized mass-action expressions yielding linear trends displaced vertically by differences in logK^c values. Using this approach, logK^c values for seven sediment samples were not significantly different. However, a significant difference in adsorption properties between one sediment sample and the fines (<0.063 mm) of another could be demonstrated despite the fines requiring a different reaction stoichiometry. Estimates of logK^c uncertainty were improved by capturing all data points within experimental errors. The mass-action expression plots demonstrate that applying models outside the range of conditions used in model calibration greatly increases potential errors.

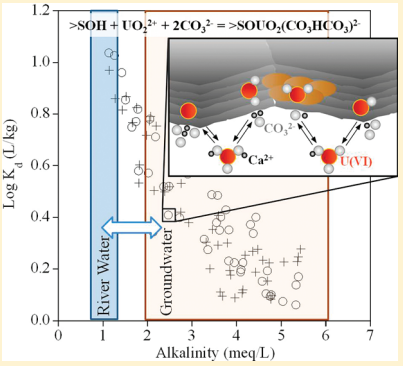

INTRODUCTION

Obtaining reliable simulations of contaminant transport in groundwater requires not only understanding contaminant adsorption properties of aquifer sediments but whether, and the extent to which, these properties vary spatially.[1] For contaminants whose sorption is controlled by simple partitioning, spatial variability is often assessed by determining empirical constants such as distribution coefficients (K_d).[1,2] The extent of adsorption of many inorganic contaminants varies with chemical conditions and, therefore, any parameters used to quantify the extent of adsorption must account for chemical variability.[3] This complicates assessment of spatial variations in adsorption properties of the sediments themselves. Previous work to assess spatial variability has focused on relating differences in contaminant adsorption to measurable sediment properties such as extractable metal concentrations, surface area, mineralogy, etc.[4−8]

The surface complexation modeling (SCM) approach has been shown to be a simple and effective approach for describing the impact of variable chemical conditions on metal and metalloid ion adsorption on soils and sediments.[9−13] Adsorption is represented as the minimum number of chemical reactions between the adsorbing solute(s), surface sites, and other species known to influence the extent of adsorption over a relevant range of chemical conditions.[14] The SCM approach should also be capable of assessing differences in adsorption properties of aquifer sediments by evaluating similarities or differences in the conditional equilibrium constant (K^c) if uncertainty can be determined adequately.

Uranium(VI) adsorption is well suited for an examination of the utility of the SCM approach to assess differences in adsorption properties of site-specific sediments.[9] The SCM approach has been used in reactive transport simulations of U(VI) and results are sensitive to the logK^c value describing U(VI) adsorption.[11,15−18] In the alkaline pH range, U(VI) forms a variety of aqueous complexes with carbonate and calcium whose predominance changes with changing pH, and carbonate and calcium concentrations.[18−22] Uranium(VI)−carbonato surface complexes are known to form at some mineral surfaces.[23] Thus, the extent of U(VI) adsorption varies considerably with variable carbonate concentration, pH, and calcium concentration.[20,24−26] This chemical variability greatly complicates distinguishing differences in adsorption properties of sediments.

The objective of this paper was to demonstrate a new approach for quantifying differences in U(VI) adsorption properties of sediment samples. To accomplish this, the time required to achieve equilibrium adsorption was determined despite long-term increases in uranium concentrations. Large differences

Received: January 3, 2011
Accepted: August 19, 2011
Revised: August 18, 2011
Published: September 16, 2011

Table 1. Elevation, Surface Area, Total and Adsorbed Uranium, and LogK^c Based on Reaction 1 for IFRC Sediments and the Weighted Average Used in Modeling "All Data"[a]

sample	elevation (m above sea level)	surface area <2 mm (m^2/g)	surface area fines[b] (m^2/g)	weight % of fines[b,c]	total U[d] (nmol/g)	adsorbed U[e] (nmol/g)	log$K^{c,f}$	logK^c FITEQL stdev[g]
2−26	105.8−107.3	11.7	14.6	21.1	12.2	2.5	21.59 ± 0.18	0.05
2−27	106.1−107.3	13.4	18.4	10.2	26.2	11.5	21.76 ± 0.19	0.06
2−30	106.4−107.3	13.3	16.4	18.1	46.5	18.3	21.68 ± 0.12	0.08
2−31	106.5−107.3	12.1	19.7	6.1	10.8	3.1	21.76 ± 0.24	0.05
3−31	106.7−107.6	11.7	16.5	10.1	16.1	8.2	21.57 ± 0.13	0.07
3−32	106.3−107.3	11.6	13.9	12.5	21.2	8.5	21.49 ± 0.12	0.05
SWC	102.6−108.0	14.1	24.0	27.2	12.2	4.4[h]	21.61 ± 0.19	0.05
all data[i]	102.6−108.0	12.6[j]	18.2[j]	15.8[j]	18.9[j]	7.5[j]	21.64 ± 0.36	0.03

[a] For errors in surface area and uranium measurements see SI Table S2. [b] Fines refer to the <0.063 mm size fraction. [c] Determined by wet sieving. [d] Determined by gamma-spectrometry on <2 mm sediment samples. [e] Determined by bicarbonate extraction on <2 mm sediment samples. [f] Reaction 1, logK_c uncertainty calculated by manually fitting data, see text. [g] Reaction 1, standard deviation calculated by FITEQL propagation of errors. [h] SWC <0.063 mm U_{ads} =9.76 nmol/g. [i] 2−26, 2−27, 2−30, 2−31, 3−31, 3−32, and SWC <2 mm data modeled together. [j] Weighted average based on experimental data used to obtain fit.

in U(VI) adsorption, owing to variable chemical conditions, were accounted for by examining trends in experimental U(VI) adsorption between different samples. Uncertainties in equilibrium adsorption model parameters, here, the conditional equilibrium constant for the adsorption reaction, were quantified. Uncertainties resulting from imperfect descriptions of the impact of variable chemical conditions were accounted for in addition to uncertainties propagating from random analytical errors.

MATERIALS AND METHODS

Site and Sample Collection. Six individual wells located across the ∼2100 m^2 Hanford 300-Area Integrated Field Research Challenge (IFRC) site were selected for study due to their spatial distribution. Close neighbor wells or cluster wells (2−26 and 2−27; 2−30 and 2−31; 3−31 and 3−32) are spaced approximately 2 m apart while the clusters are approximately 30 m from each other (see site map in Supporting Information (SI), Figure S1). Grab samples of sediment were collected during the drilling of wells, discretized to 2 foot depth intervals, air-dried, and dry sieved to <2 mm. A continuous core from well 2−5 was examined to define the seasonally saturated smear-zone in which higher levels of adsorbed uranium accumulate due to repeated wetting and drying cycles.[27−29] Once the smear-zone elevation was defined, material from this elevation range was isolated for each of the six individual wells mentioned above (See Table 1 for specific elevations). For five of the six individual wells (2−26, 2−30, 2−31, 3−31, and 3−32), in addition to the smear-zone sample, a sample was also collected from the deeper permanently saturated aquifer (97−103 m above sea level) to establish background total and adsorbed uranium concentrations. Finally, the <2 mm size fraction sediment collected from the smear-zone of 31 wells across the site (See SI Figure S1) was mixed together into a site-wide composite (SWC).

Sediment Characterization. Each smear-zone sediment sample was wet-sieved to determine particle size distribution. Samples were also dry sieved to isolate the <0.063 mm size fraction (herein referred to as "fines") for further study. Surface areas were measured, in duplicate, on both the original <2 mm and dry sieved fines of each sample using N_2 adsorption at 77.3 K (Micromeritics Tristar 3000). Samples (∼2 g) were degassed at 105 °C for 3−5 days and the 5-point BET method applied to adsorption curves with C parameters between 100 and 300.[30] X-ray diffractograms were collected on the fines using a Phillips X-ray diffractometer between 4 and 70 degrees 2 theta.

Total uranium was measured via nondestructive gamma-spectrometry. ^{238}U was determined by measurement of the ^{234}Th daughter 63 keV gamma ray emission line on each <2 mm sample, assuming secular equilibrium in the sample.[31] Adsorbed uranium was determined via bicarbonate extraction. The <2 mm sediment (50 g/L) and fines of SWC (15 g/L) were reacted with a solution of 2.8 mM Na_2CO_3 and 14.4 mM $NaHCO_3$ at pH 9.5 and 20 meq/L alkalinity. Experimental studies on Hanford and other sediments have shown that determinations of adsorbed uranium by bicarbonate extraction are equal to those determined by ^{233}U isotopic exchange.[20,32] Duplicate reaction bottles were mixed on an orbital shaker table and intermittently subsampled by filtering (0.45 μm, PVDF) 3 mL of supernatant after settling. Samples were collected up to 9400 h (56 weeks) and U(VI) concentrations measured using a Chemchek KPA-11 kinetic phosphorescence analyzer (KPA). Major solution cations were measured via inductively coupled plasma-optical emission spectroscopy (ICP-OES) using a Thermo Scientific iCAP 6500.

Citrate bicarbonate dithionite (CBD) extractions were performed in duplicate on both the <2 mm (5 g) and fines (2 g) of each sample per the modified method detailed by Loppert and Inskeep,1996 at 80 °C and pH 7.[33] The <2 mm size fraction was also ground to pass through a 0.063 mm sieve (2 g) and extracted with CBD. Ammonium oxalate extractions in the dark (AOD) were carried out as described in Chao and Zhou, 1983 in duplicate on the <2 mm samples (5 g) and fines (1 g) at ambient temperature and pH 3.[34] Aqueous iron concentrations were measured by ICP-OES.

Equilibrium Adsorption Experiments. A series of five artificial groundwaters (AGWs) were designed to mimic the 300-Area groundwater during its seasonal fluctuations due to mixing of river water and groundwater. These waters have been described elsewhere and compositions are given in SI Table S1.[18] Briefly, solution calcium (0.5 mM), magnesium (0.5 mM), and potassium (0.15 mM) concentrations were maintained while alkalinity ($NaHCO_3$) was varied between 0.5 and 6 meq/L in equilibrium with the atmosphere (pH 7.8−8.1). Sodium salts (nitrate and sulfate) were added as necessary to maintain an ionic strength of 10 mM. The <2 mm size fraction of each material as well as

the SWC fines were mixed with AGW in polycarbonate centrifuge tubes on an end-overend rotator at ambient temperature. All experiments were performed in duplicate at either 100 g/L (AGW 1, 2, 3) or 1000 g/L (AGW 3, 4, 5) and tubes sacrifice-sampled at various time points up to 7000 h (42 weeks). While experiments began at atmospheric pCO_2, no attempt was made to control the pCO_2 in the head space of each tube. At the time of sampling, the lid was quickly removed and replaced with one outfitted with a pH electrode to determine suspension pH while minimizing changes in pCO_2. The tube was then centrifuged, supernatant filtered, and the solution uranium and cation concentrations measured. Alkalinity was determined on the filtered solution by titration with standardized sulfuric acid (Fisher Scientific).

Modeling. Conditional equilibrium constants (K^c) for surface complexation adsorption reactions with no electrostatic term were computed from the experimental data by nonlinear, least-squares optimization using FITEQL.[35] The adsorbed U(VI) concentration at equilibrium was calculated from the original adsorbed U(VI) concentration for each sample, determined using bicarbonate extraction (Table 1), minus the dissolved concentration. The site concentration was calculated from the solid−liquid ratio, specific surface area (Table 1), and an assumed site density of 3.84 μmol/m^2.[3] In the generalized composite approach to surface complexation modeling, an average, generic surface site (SOH) is used to represent adsorption onto the complex assemblage of minerals in field samples. Carbonate concentrations were computed from measured pH and alkalinity values. These values, along with the concentrations of calcium, magnesium, sodium, potassium, and sulfate, were used to compute aqueous U(VI) speciation in the fitting. Nitrate concentrations were calculated to achieve charge balance. Experimental errors used in the fitting procedure were 10% for H^+, 3% for carbonate, 10% for adsorbed U(VI), 3% for dissolved U(VI), 10% for site concentration, and 5% for all other dissolved concentrations. The basis for each error assumption is described in SI Table S2. Aqueous U(VI) speciation was computed using previously reported thermodynamic data.[15] Experimental data collected at 2000 h (12 weeks) of equilibration were used in the fitting. Each individual sample was modeled separately and the 2000 h data for all samples were then modeled together to produce what is referred to as the "all data" model.

RESULTS AND DISCUSSION

Sediment Characterization. Surface areas of the <2 mm sediment varied between 11.5 and 14.1 m^2/g. The average specific surface area, calculated by averaging surface area values associated with each data point used in the "all data" fitting procedure, was 12.6 m^2/g (Table 1). The surface area of the fines (<0.063 mm) ranged from 13.9 to 24.0 m^2/g and constituted 6−27% by weight of the <2 mm material. The fine-grained material accounts for 10−26% of the surface area of each individual well sample and 46% of the surface area of the site-wide composite (SWC).

Total uranium varied between 11 and 47 nmol/g for the smear-zone sediment samples (Table 1). The highest and lowest total uranium concentrations occurred in sediment collected 2 m apart in one of the three well clusters (2−30 and 2−31). Similar variations over short spatial distances were observed for another well cluster (2−26 and 2−27) while the third showed less variation between samples (3−31 and 3−32). The deep saturated-zone samples contained much less total uranium with an average of 7.6 nmol/g, near the average crustal abundance of uranium of 8−12 nmol/g.

Previous spectroscopic evaluations of sediment from the Hanford formation of the 300-Area near this field site have shown only the presence of oxidized hexavalent uranium U(VI).[29,36,37] Therefore, uranium described herein is assumed to be U(VI). Adsorbed U(VI) ranged from 2.5 to 18.3 nmol/g accounting for 20−61% of the total uranium in each sample. During bicarbonate extraction, dissolved concentrations of uranium increased rapidly for the first 24 h and then more slowly out to 1700 h after which concentrations remained steady. The slow progression toward complete desorption is consistent with previous findings of mass-transfer diffusion limitations on contaminant release at this site.[15,16,38,39] A positive linear correlation exists between total and adsorbed uranium. Similar to the total uranium concentrations, the highest and lowest adsorbed uranium concentrations occurred in sediment collected 2 m apart (2−30 and 2−31, see SI Figure S2). No discernible pattern is evident between extractable uranium and sample location. The spatial variations in adsorbed uranium (and total uranium) observed in the smear-zone were not evident in the deep saturated-zone samples. For the deep saturated-zone samples, the average adsorbed uranium was 1.1 nmol/g; representing between 4.3 and 12.6% of the total uranium. Adsorbed uranium in samples from the deep saturated-zone may represent natural background levels of adsorbed uranium similar to other field sites such as Rifle, CO at 1.4 nmol/g and Naturita, CO at 0.87 nmol/g.[7,26]

Mineralogy and iron extractions of sediment samples suggest similar solid-phase compositions across the field site. XRD of fines showed each sample was comprised primarily of quartz and plagioclase with moderate contributions from pyroxene and minor (<5%) abundance of poorly crystalline clays composed of illite, kaolinite, and extremely poorly crystalline smectite. CBD extractions of the <2 mm smear-zone sediments yielded between 3.6 and 6.2 μmol/m^2 iron while AOD released between 5.5 and 10.3 μmol/m^2 (SI Table S3). Extractions of the fines resulted in approximately two times more iron released by each method when normalized to surface area. Details of the limitations of these extractions can be found in the SI. Though small differences in extractable iron were observed between samples, no correlations could be found between adsorbed uranium or surface area and the iron extracted by either AOD or CBD. In addition, no significant correlation could be found between the amount of adsorbed uranium on a sediment and its surface area or weight percentage of fines.

Equilibrium Adsorption Experiments. Desorption experiments were carried out at 100 g/L for groundwaters with low alkalinities (0.5−2 meq/L). However, at higher alkalinities (>2 meq/L), 100% of the adsorbed uranium was extracted at this suspension density within 700 h. Therefore, higher alkalinity experiments were conducted at 1000 g/L. At low suspension densities (100 g/L), dissolved uranium concentrations increased rapidly for the first 24 h and then increased at a slower rate for duration of the experiments (Figure 1a). In these systems, between 52 and 94% of the adsorbed uranium was released after 2000 h. Changes in pH, alkalinity, and calcium concentrations were observed throughout the duration of the experiments (see Figure 1a). The initial chemical changes (24−72 h) can be attributed to dissolution of aquifer salts, which precipitated when the sediment was dried, and ion exchange reactions.[16] However, later chemical changes are likely due to a combination of slow

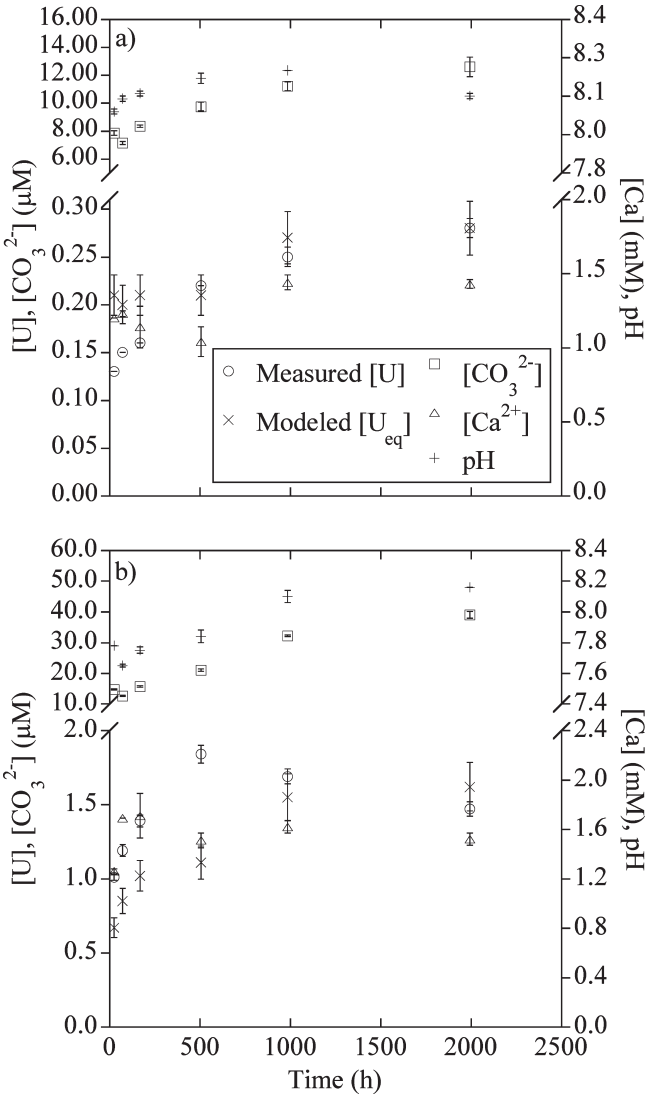

Figure 1. Measured dissolved uranium concentrations, "free" carbonate concentrations in the form of CO_3^{2-} and modeled equilibrium aqueous uranium concentrations; dissolved calcium concentrations and pH plotted on the secondary *y*-axis for sample SWC <2 mm in AGW-2, 100 g/L (a) and AGW-4, 1000 g/L (b). Error bars for measured variables represent differences between experimental duplicates while error bars for modeled [U] are based on logK^c uncertainty (Table 1).

incongruent alumino-silicate mineral dissolution, evidenced by the continued release of silicon, and possible aerobic respiration.[40] While organic content in these sediments is low (0.05–0.2% by weight), the impact of microbial activity, observed previously in column experiments, is suggested by increases in alkalinity.[18] Therefore, at 100 g/L, aqueous chemical conditions influencing uranium(VI) speciation changed steadily throughout the experiments.

Less extensive changes in solution chemistry were observed in experiments conducted at higher suspension density (1000 g/L). Uranium concentrations increased rapidly during the initial 24 h of the experiments, slowly increased out to about 500 h, and then remained relatively constant for the duration of the experiments (Figure 1b). At higher suspension densities, 32–48% of the adsorbed uranium was released. Alkalinity, pH and calcium concentrations fluctuated initially and stabilized after ~500 h. While none of the AGWs were oversaturated with respect to calcite, once placed in contact with the sediments, solutions were found to be oversaturated as soon as the first sampling point at 24 h. For example, in the SWC AGW 2 system at 100 g/L shown in Figure 1a, calcite ion activity product increased from 0.04 to 0.29 over 2,000 h of reaction and from 0.32 to 0.79 for SWC in AGW 4 at 1000 g/L. These values are similar to those reported elsewhere for U(VI) contaminated calcareous sediments.[7,20] It is critically important to allow for this oversaturation in modeling uranium adsorption as calcium readily forms solution complexes with uranium and carbonate and strongly impacts solid/solution partitioning of uranium.[7]

Modeling the Impact of Variable Chemistry. Our objective was to develop an SCM that accounted for the impact of variable chemical conditions on equilibrium U(VI) adsorption so that the U(VI) adsorption properties of individual sediment samples could be compared. The optimal SCM was determined by fitting experimentally measured U(VI) equilibrium adsorption–desorption on different sediment samples across the range of chemical conditions applicable to the study area. Nine reactions (SI Table S4) differing in stoichiometric relationships between U(VI), carbonate, and H^+ were tested to find which reaction (or combination of reactions) achieved the best possible description of the impact of variable chemical conditions on U(VI) adsorption on these sediment samples (see SI for a description of the assessment of the quality of fit for each reaction).

The best fit for all <2 mm sediment samples was achieved with Reaction 1 while the SWC fines were best fit by Reaction 2.

$$> SOH + UO_2^{2+} + 2CO_3^{2-} => SOUO_2(CO_3HCO_3)^{2-} \quad (1)$$

$$> SOH + UO_2^{2+} + 2CO_3^{2-} => SOUO_2(CO_3)_2^{3-} + H^+ \quad (2)$$

For each individual data set, model-calculated and measured K_d values agreed within experimental uncertainties for 80% of the data points. Data points where model-calculated and measured adsorption fell out of the range of experimental errors showed no discernible trend with chemical conditions. The model captures the decreasing trends in U(VI) adsorption with increasing alkalinity (Figure 2). This trend is significant as lower alkalinity Columbia River water mixes with groundwater of higher alkalinity during high river stages.[27,28] As will be shown, scatter in the measured and model-calculated U(VI) adsorption results primarily from variable chemical conditions other than alkalinity.

For all samples, attempts to fit a second reaction to the data failed as long as Reaction 1 (or Reaction 2 for the SWC fines) was included, indicating that this reaction by itself accounted for most of the chemical variability observed in the data. Similarly, no improvement in fits was obtained using single-reaction two-site models, where a portion of the total sites were allowed to bind more strongly than the remainder of the sites.[24,41] Bond *et al.*, 2008 found that two reactions (Reactions 7 and 8 in SI Table S4) provided the best fit for samples from the vadose-zone of the 300-Area.[20] This sample set included sediments containing uranium mineral precipitates and showing clear signs of alteration, likely resulting from the highly acidic and alkaline solutions discharged to the shallow pits in this area.[20,36,37,42] Examination of the impact of the assumed site density on the conditional constant

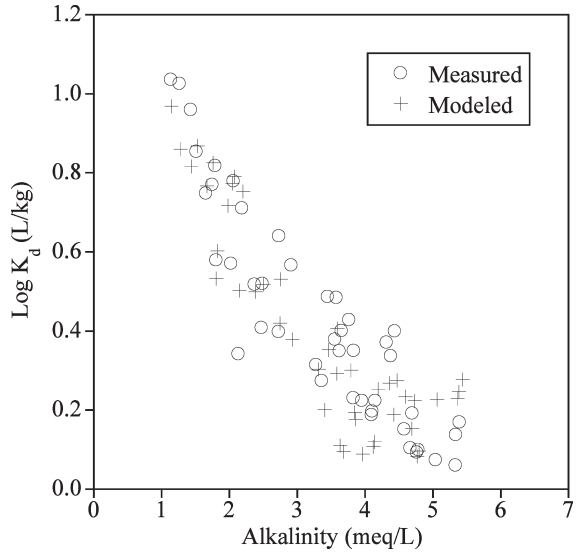

Figure 2. U(VI) adsorption, expressed as the ratio of adsorbed (mol/kg) and dissolved (mol/L) U(VI) concentrations, on IFRC samples. Model-calculated U(VI) adsorption used the best-fit SCM for "all data" based on Reaction 1.

revealed that they are inversely proportional until the site density approaches the initial adsorbed U(VI) concentration and the assumed site density does not influence which reaction provides the best fit (Table S5, Figure S3, and SI discussion). Given the low adsorbed U(VI) concentrations applicable to the study site (<1.4 nmol/m^2), U(VI) adsorption on sediments may be dominated by a small percentage of total sites with high affinity for U(VI). In that case, a lower logK^c value might be required at higher adsorbed U(VI) concentrations. The proportionality between site density and K^c shows that the approach used here to determine differences in U(VI) binding by sediments cannot distinguish between differences in the intrinsic U(VI) binding properties of adsorption sites and small differences in site density between samples.

In order to understand the factors controlling continual changes in uranium concentrations observed during the experiments, the SCM for each sample was used to compute the equilibrium uranium concentration at each time point based on the observed chemical conditions. Uranium adsorption equilibrium was achieved within 500 h for SWC 100 g/L experiments as indicated by the agreement between calculated equilibrium solution concentrations and measured concentrations (Figure 1a). Subsequently, uranium concentrations remained at adsorption equilibrium while chemical conditions (e.g., calcium concentrations) evolved in a manner that increased the equilibrium U(VI) concentration. In the SWC 1000 g/L experiment, uranium concentrations were above those expected for adsorptive equilibrium for the first 500 h of the experiment (Figure 1b). At this high solid-to-liquid ratio, uranium concentrations were evidently affected by irreversible processes likely associated with the history of the sample.[27,28,16] Adsorptive equilibrium was achieved within 1000 h, after which time uranium concentrations remained at equilibrium for the duration of the experiment. Similar results were obtained for experiments conducted with the other sediment samples at both suspension densities.

Standard deviations estimated by FITEQL account for the impact of analytical errors on fitted conditional equilibrium constants. An additional source of uncertainty derives from possible incomplete description of the impact of variable chemical conditions provided by the reaction or reactions chosen to fit the data.[14] This additional source of uncertainty in the logK^c values was estimated by adjusting the logK^c value up and down until the "logK^c envelope" captured all experimental data points (Table 1). For all samples, the logK^c envelope uncertainty was larger than the FITEQL standard deviation. This is particularly clear for the "all data" fit. The standard deviation computed from propagation of experimental errors (0.03) decreased in proportion to the square root of the increase in data points used in the fit.[12] In contrast, the logK^c envelope uncertainty increased (0.36) as one would expect when fitting data from sediment samples with apparent differences in logK^c values.

Comparing Adsorption Properties of Sediment Samples. In order to determine whether there are significant differences in U(VI) adsorption properties of sediment samples one must first minimize variability and scatter in measured and model-calculated adsorbed U(VI) concentrations owing to aqueous chemical conditions (e.g., Figure 2). This can be achieved by rearranging mass-action expressions for the adsorption reactions as linear functions of the log of the activity of the aqueous species that control U(VI) speciation: UO_2^{2+}, CO_3^{2-}, and H^+. For Reaction 1 the expressions are as follows:

$$\log \frac{[\mathrm{SOUO_2(CO_3HCO_3)^{2-}}]}{[\mathrm{SOH}](\mathrm{UO_2^{2+}})} = \log(\mathrm{R_1CO_3}) = \log K^c + 2\log(\mathrm{CO_3^{2-}}) \quad (3)$$

$$\log \frac{[\mathrm{SOUO_2(CO_3HCO_3)^{2-}}]}{[\mathrm{SOH}](\mathrm{CO_3^{2-}})^2} = \log(\mathrm{R_1UO_2}) = \log K^c + \log(\mathrm{UO_2^{2+}}) \quad (4)$$

$$\log \frac{[\mathrm{SOUO_2(CO_3HCO_3)^{2-}}]}{[\mathrm{SOH}](\mathrm{UO_2^{2+}})(\mathrm{CO_3^{2-}})^2} = \log(\mathrm{R_1H}) = \log K^c \quad (5)$$

where square brackets symbolize concentrations (surface species, in mol/L) and parentheses symbolize activity (aqueous species). Plots of the experimental data, expressed as the quotients on the left-hand side of eqs 3 and 4 against log carbonate and log uranyl activity, should yield linear trends with slopes of 2 and one, respectively. Hydrogen ions do not appear in Reaction 1 so a plot of the mass-action expression on the left-hand side of eq 5 vs pH should yield horizontal trends. Samples with significantly different adsorption properties will yield parallel, linear trends separated by differences in their logK^c values. Analogous expressions can be written based on other reactions to be examined; these would have different slopes based on the stoichiometric coefficients for the applicable reaction. To the extent that the chosen reaction does not provide an adequate description of the impact of variable chemistry on adsorption, the slope of the linear trend in the experimental data will deviate from the stoichiometric coefficient.

Plots of the experimental data for sediment samples 2−27, 2−31, 3−32, and SWC using eqs 3−5 show linear trends for each sample (SI Figure S4). The overlap of data points within experimental error across the range of log carbonate, uranyl, and H^+ conditions studied indicate that these samples do not have significantly different logK^c values. Slopes of the log(R_1CO_3) vs log(CO_3) trendlines (SI Figure S4a) for 2−27, 2−31, 3−3,2 and

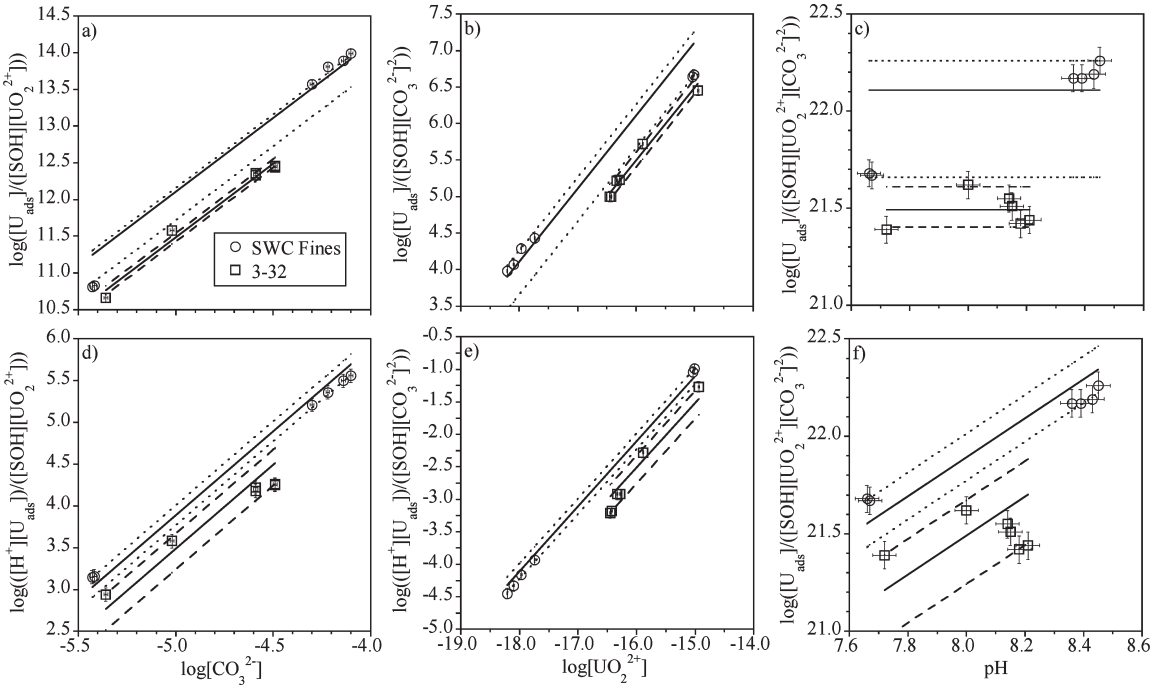

Figure 3. Experimental data plotted for 3−32 and the SWC Fines (<0.063 mm) for Reaction 1 in terms of (a) $\log R_1CO_3$ vs CO_3, (b) $\log R_1UO_2$ vs UO_2, (c) $\log R_1pH$ vs pH and for Reaction 2 in terms of (d) $\log R_2CO_3$ vs CO_3, (e) $\log R_2UO_2$ vs UO_2, (f) $\log R_2pH$ vs pH. The best-fit conditional equilibrium constant ($\log K^c$) is marked by a solid line for each sample. The uncertainty in $\log K^c$ is bounded by the dotted or dashed lines calculated by adjusting the parameter in the positive and negative direction until calculated U(VI) adsorbed concentrations agree with all measured values. Vertical and horizontal error bars represent propagation of error values assumed in modeling (SI Table S2).

SWC are 2.0, 2.2, 2.0, and 1.8, respectively, as compared to the theoretical slope of 2. Similarly, slopes of $\log(R_1UO_2)$ vs $\log(UO_2^{2+})$ trendlines (SI Figure S4b) are 1.0, 0.9, 1.0, and 1.1, respectively (theoretical slope equals 1); slopes of $\log(R_1pH)$ vs pH trendlines (SI Figure S4c) are 0.1, 0.4, 0.1, and −0.5, respectively, (theoretical slope equals 0). Thus, Reaction 1 captures most of the impact of the variability in chemistry on uranium adsorption for these samples.

Adsorption properties of sediment sample 3−32, which exhibited the lowest U(VI) adsorption $\log K^c$ (Table 1), were compared with those of the SWC fines using mass-action expressions for Reaction 1, the best fit for sample 3−32, and Reaction 2, the best fit for the fines (SI Table S4). In all mass-action plots, trends in the experimental data for the SWC fines fall above those for sample 3−32 in excess of experimental errors over the range of chemical conditions examined (Figure 3). Also, trends calculated from $\log K^c$ values for the SWC fines exceed those for sample 3−32 even when the maximum and minimum $\log K^c$ values ($\log K^c$ envelope) for the SWC fines and sample 3−32 and are considered. Larger uncertainty values are necessary to capture all data points when the surface complexation model does not describe the impact of variable chemistry well. For sample 3−32, the uncertainty in $\log K^c$ using Reaction 1 is 0.12 but increases to 0.25 with Reaction 2. Conversely, the SWC fines uncertainty for Reaction 1 is 0.45 but decreases to 0.12 with Reaction 2. Using either reaction, the SWC fines have a statistically significant higher U(VI) adsorption affinity than sediment sample 3−32 (Tables 1 and SI S4). Experimental trends overlapped within experimental errors along the range of chemical conditions studied for all other pairs of sediment samples from the site (SI Figure S4). Thus, no significant difference in U(VI) adsorption properties between these sediment samples could be established.

Ratios of K^c values for the SWC fines to sample 3−32 are 4 and 3 for Reaction 1 and 2, respectively (SI Table S4). The maximum difference in K^c values among the IFRC <2 mm sediment samples for Reaction 1 is a factor of 2 (Table 1). Based on this set of samples, the minimum difference in K^c values needed to establish a significant difference in U(VI) adsorption properties over and above differences in U(VI) adsorption owing to variable chemical conditions is a factor of 3 to 4. For comparison, adsorbed U(VI) concentrations vary by a factor of 30 over the range of chemical conditions studied (Figure 2). The implications of the lack of differences in $\log K^c$ values to U(VI) transport at the site will be important to understand. Sediments examined in this investigation were collected over relatively coarse vertical intervals (Table 1). Examinations conducted at a finer scale may reveal greater variability.

Implications. Some additional observations about $\log K^c$ uncertainty can be made using this mass-action based analysis. Disparities between slopes of the experimental trends and the theoretical slopes increase the uncertainty in the $\log K^c$ value. This is especially clear in plots of $\log(R_1pH)$ and $\log(R_2pH)$ vs pH, where the experimental trends suggest a slope of 0.1 for sample 3−32 and a slope of 0.7 for the SWC fines (Figure 3c and f with theoretical slopes of 0 and 1, respectively). Where such disparities exist, applying the SCM outside of the range of chemical conditions used for model calibration can result in errors in computed adsorbed U(VI) that exceed those that can be estimated from the experimental data. A reliable comparison of U(VI) adsorption properties of sediment samples can only be made if the range of chemical conditions over which the

properties are determined coincide. The appropriate range of chemical conditions for such comparisons and for assessment of SCM applicability is best defined in terms of the species that comprise aqueous and surface complexes: free UO_2^{2+}, H^+, and CO_3^{2-}. Using these species will take into account variations in concentrations of other solutes like calcium and magnesium that form aqueous U(VI) species.

The lack of significant differences in logK^c values of sediment samples collected across the Hanford IFRC site may be related to the lack of mineralogical differences observed. Spectroscopic studies suggest that dominant U(VI) surface complexes form on quartz and phyllosilicate minerals.[43] Determining differences in these ubiquitous minerals across a heterogeneous field site could prove exceedingly difficult. In a study carried out in a quartz-sand aquifer, a significant correlation was found between surface area normalized Pb^{2+} adsorption (0.7−1.2 μmol/m^2) and extractable iron and aluminum with similar results for Zn^{2+} (0.03−0.07 μmol/m^2).[5] This is expected given the high adsorption densities and importance of aluminum-substituted goethite coatings on quartz surfaces in controlling adsorption properties in the absence of organic or inorganic carbon.[5,44] Under these conditions, traditional chemical extractions may provide a reliable estimate of variability in the abundance of the constituents and, thereby, their absorptive capacity and variability. At the Hanford IFRC site, with carbonate mineral complexation of uranium and the diffuse distribution of clays and clay coatings throughout the aquifer, characterizing spatial variability of adsorption properties of uranium requires more thorough study.

■ ASSOCIATED CONTENT

Supporting Information. Discussion of iron extractions, model fitting, and assumed site density impacts on logK^c. Tables S1−S5: AGW composition, SCM reactions and assumed errors, extractable iron data and site density parameters. Figures S1−S4: Site map, adsorbed uranium depth profile, assumed site density impacts of logK^c and additional mass-action plots. This material is available free of charge via the Internet at http://pubs.acs.org.

■ AUTHOR INFORMATION

Corresponding Author

*Phone: 650-329-4529; fax: 650-329-4545; e-mail: dlstoliker@usgs.gov.

■ ACKNOWLEDGMENT

Funding for this work was provided by the U.S. Department of Energy Office of Science, Subsurface Biogeochemical Research program, through the Hanford 300-Area IFRC. Additional funding came from the U.S. Geological Survey through the Hydrologic Research and Development program. Technical assistance from Chris Fuller in the measurement of total uranium is gratefully acknowledged. We thank Tracie Conrad and James Hein for XRD analyses. Discussions with Roy Haggerty, Chongxuan Liu, and Jun Yin along with reviews by Gary Curtis, James Davis, and four anonymous reviewers improved the quality of this manuscript.

■ REFERENCES

(1) Allen-King, R. M.; Divine, D. P.; Robin, M. J. L.; Aldredge, J. R.; Gaylord, D. R. Spatial distributions of perchloroethylene reactive transport parameters in the Borden Aquifer. *Water Resour. Res.* **2006**, *42*, W01413, DOI: 10.1029/2005WR003977.

(2) Rajaram, H. Time and scale dependent effective retardation factors in heterogeneous aquifers. *Adv. Water Resour.* **1997**, *20*, 217–229.

(3) Davis, J. A.; Kent, D. B. Surface complexation modeling in aqueous geochemistry. In *Mineral-Water Interface Geochemistry Vol 23*; Hochella, M. F., White, A. F., Eds.; Mineralogical Society of America: Washington, DC, 1990; pp 177−260.

(4) Davis, J. A.; Fuller, C. C.; Coston, J. A.; Hess, K. M.; Dixon, E. *Spatial Heterogeneity of Geochemical and Hydrologic Parameters Affecting Metal Transport in Ground Water*; U.S. Environmental Protection Agency: Washington, DC, 1993; EPA/600/S-93/006.

(5) Fuller, C. C.; Davis, J. A; Coston, J. A.; Dixon, E. Characterization of metal adsorption variability in a sand and gravel aquifer, Cape Cod, Massachusetts, U.S.A. *J. Contam. Hydrol.* **1996**, *22*, 165–187.

(6) Hull, L. C.; Grossman, C.; Fjeld, R. A.; Coates, J. T.; Elzerman, A. W. Hybrid empirical-theoretical approach to modeling uranium adsorption. *Appl. Geochem.* **2004**, *19*, 721–736.

(7) Hyun, S. P.; Fox, P. M.; Davis, J. A.; Campbell, K. M.; Hayes, K. F.; Long, P. E. Surface complexation modeling of U(VI) adsorption by aquifer sediments from a former mill tailing site at Rifle, Colorado. *Environ. Sci. Technol.* **2009**, *43*, 9368–9373.

(8) Sharif, M. S. U; Davis, R. K.; Steele, K. F.; Kin, B.; Hays, P. D.; Kreese, T. M.; Fazio, J. A. Surface complexation modeling for predicting solid phase arsenic concentrations in the sediments of the Mississippi River Valley alluvial aquifer, Arkansas, USA. *Appl. Geochem.* **2011**, *26*, 496–504.

(9) Miller, A. W.; Rodriguez, D. R.; Honeyman, D. B. Upscaling sorption/desorption processes in reactive transport models to describe metal/radionuclide transport: A critical review. *Environ. Sci. Technol.* **2010**, *44*, 7996–8007.

(10) Curtis, G. P.; Davis, J. A.; Naftz, D. L. Simulation of reactive transport of uranium (VI) in groundwater with variable chemical conditions. *Water Resour. Res.* **2006**, *42*, W04404, DOI: 10.1029/2005WR003979.

(11) Ma, C.; Zheng, C.; Prommer, H.; Greskowiak, J.; Liu, C.; Zachara J. A field-scale reactive transport model for U(VI) migration influenced by coupled multirate mass transfer and surface complexation reactions. *Water Resour. Res.* **2010**, *46*, W05509; DOI: 10.1029/2009WRR008168.

(12) Dzombak, D. A.; Morel, F. M. M. *Surface Complexation Modeling: Hydrous Ferric Oxide*; Wiley-Interscience: New York, 1990.

(13) Westall, J. C.; Jones, J. D.; Turner, G. D.; Zachara, J. M. Models for association of metal ions with heterogeneous environmental sorbents. 1. Complexation of Co(II) by leonardite humic acid as a function of pH and $NaClO_4$ concentration. *Environ. Sci. Technol.* **1995**, *29*, 951–959.

(14) Davis, J. A.; Coston, J. A.; Kent, D. B.; Fuller, C. C. Application of the surface complexation concept to complex mineral assemblages. *Environ. Sci. Technol.* **1998**, *32*, 2820–2828.

(15) Liu, C.; Zachara, J. M.; Qafoku, N. P.; Wang, Z. Scale-dependent desorption of uranium from contaminated subsurface sediments. *Water Resour. Res.* **2008**, *44*, W08413, DOI: 10.1029/2007WR006478.

(16) Liu, C.; Shi, S.; Zachara, J. M. Kinetics of uranium(VI) desorption from contaminated sediments: Effect of geochemical conditions and model evaluation. *Environ. Sci. Technol.* **2009**, *43*, 6560–6566.

(17) Greskowiak, J.; Prommer, H.; Liu, C.; Post, V. E. A.; Ma, R.; Zheng, C.; Zachara, J. M. Comparison of parameter sensitivities between laboratory and field-scale model of uranium transport in a dual domain, distributed rate reactive system. *Water Resour. Res.*, **2010**, *46*, W05509, DOI: 10.1029/2009WR008781.

(18) Yin, J.; Haggerty, R.; Stoliker, D. L.; Kent, D. B.; Istok, J. D.; Greskowiak, J.; Zachara J. M. Transient groundwater chemistry near a river: Effects on U(VI) transport in laboratory column experiments. *Water Resour. Res.* **2011**, 47, DOI: 10.1029/2010WR009369.

(19) Dong, W.; Brooks, S. C. Determination of the formation constants of ternary complexes or uranyl and carbonate with alkaline

earth metals (Mg^{2+}, Ca^{2+}, Sr^{2+}, and Ba^{2+}) using anion exchange method. *Environ. Sci. Technol.* **2006**, *40*, 4689–4695.

(20) Bond, D. L.; Davis, J. A.; Zachara, J. M. Uranium(VI) release from contaminated vadose zone sediments: estimation of potential contributions for dissolution and desorption. In *Adsorption of Metals by Geomedia II: Variables, Mechanisms and Model Applications*; Barnett, M. O., Kent, D. B., Eds.; Elsevier: Amsterdam, 2008; pp 375−416.

(21) Fox, P. M.; Davis, J. A.; Zachara, J. M. The effect of calcium on aqueous uranium(VI) speciation and adsorption to ferrihydrite and quartz. *Geochim. Cosmochim. Acta* **2006**, *70*, 1379–1387.

(22) Stewart, B. D.; Mayes, M. D.; Fendorf, S. Impact of uranyl-calcium-carbonato complexes on uranium(VI) adsorption to synthetic and natural sediments. *Environ. Sci. Technol.* **2010**, *44*, 928–934.

(23) Bargar, J. R.; Reitmeyer, R.; Lenhart, J. J.; Davis, J. A. Characterization of U(VI)-carbonato ternary complexes on hematite: EXAFS and electrophoretic mobility measurements. *Geochim. Cosmochim. Acta* **2000**, *64*, 2737–2749.

(24) Waite, T. D.; Davis, J. A.; Payne, T. E.; Waychunas, G. A.; Xu, N. Uranium (VI) adsorption to ferrihydrite: Application of a surface complexation model. *Geochim. Cosmochim. Acta* **1994**, *58*, 5465–5478.

(25) Barnett, M. O. Adsorption and transport of U(VI) in subsurface media. *Soil Sci. Soc. Am. J.* **2000**, *64*, 908–917.

(26) Davis, J. A.; Meece, D. E.; Kohler, M.; Curtis, G. P. Approaches to surface complexation modeling of uranium(VI) adsorption on aquifer sediments. *Geochim. Cosmochim. Acta* **2004**, *68*, 3621–3641.

(27) Zachara, J. M.; Davis, J. A.; Liu, C.; McKinley, J. P.; Qafoku, N.; Wellman, D. M.; Yabusaki, S. *Uranium Geochemistry in Vadose Zone and Aquifer Sediments From the 300-Area Uranium Plume*; United States Department of Energy: Washington, DC, 2005; PNNL-15121.

(28) McKinley, J. P.; Zachara, J. M.; Wan, J.; McCready, D. E.; Heald, S. M. Geochemical controls on contaminant uranium in vadose Hanford formation sediments at the 200 Area and 300 Area, Hanford Site, Washington. *Vadose Zone J.* **2007**, *6*, 1004–1017.

(29) Singer, D. M.; Zachara, J. M.; Brown, G. E. Uranium speciation as a function of depth in contaminated Hanford sediments − a micro-XFR, micro-XRD, and micro- and bulk-XAFS study. *Environ. Sci. Technol.* **2009**, *43*, 630–636.

(30) Gregg, S. J.; Sing, K. S. W. *Adsorption, Surface Area, and Porosity*; Academic Press: New York, 1982.

(31) Davis, J. A.; Curtis, G. P. *Application of Surface Complexation Modeling to Describe Uranium (VI) Adsorption and Retardation at the Uranium Mill Tailings Site at Naturita, Colorado*; U.S. Nuclear Regulatory Commission: Rockville, MD, 2003; NUREG/CR-6708;.

(32) Kohler, M.; Curtis, G. P.; Meece, D. E.; Davis, J. A. Methods for estimating adsorbed uranium(VI) and distribution coefficients of contaminated sediments. *Environ. Sci. Technol.* **2004**, *38*, 240–247.

(33) Loeppert, R. H.; Inskeep, W. P. Iron. In *Methods of Soil Analysis, Part 3, Chemical Methods, SSSA Book Series No. 5*; Sparks, D. L., Ed.; Soil Science Society of America: Madison, WI, 1996; pp 639−664.

(34) Chao, T. T.; Zhou, L. Extraction techniques for selective dissolution of amorphous iron oxides from soils and sediments. *Soil Sci. Soc. Am. J.* **1983**, *47*, 225–232.

(35) Herbelin, A. L.; Westall, J. C. *FITEQL: A Computer Program for the Determination of Chemical Equilibrium Constants from Experimental Data*; Chemistry Department, Oregon State University: Corvallis, OR, 1999.

(36) Catalano., J. G.; McKinley, J. P.; Zachara, J. M.; Heald, S. M.; Smith, S. C.; Brown, G. E. Changes in uranium speciation through a depth sequence of contaminated Hanford sediments. *Environ. Sci. Technol.* **2006**, *40*, 2517–2524.

(37) Arai, Y.; Marcus, M. A.; Tamura, N.; Davis, J. A.; Zachara, J. M. Spectroscopic evidence for uranium bearing precipitates in vadose zone sediments at the Hanford 300-area site. *Environ. Sci. Technol.* **2007**, *41*, 4633–4639.

(38) Shang, J.; Liu, C.; Wang, Z.; Zachara, J. M. Effect of grain size on uranium(VI) surface complexation kinetics and adsorption additivity. *Environ. Sci. Technol.* **2011**, *45*, 6025–6031.

(39) Qafoku, N. P.; Zachara, J. M.; Liu, C.; Gassman, P. L.; Qafoku, O. S.; Smith, S. C. Kinetic desorption and sorption of U(VI) during reactive transport in a contaminated Hanford sediment. *Environ. Sci. Technol.* **2005**, *39*, 3157–3165.

(40) Blum, A. E.; Stillings, L. L. Feldspar dissolution kinetics. In *Rev. Mineral. Geochem. Vol. 31*; White, A. F., Brantley, S. L., Eds.; Mineralogical Society of America: Washington, DC, 1995; pp 291−351.

(41) Kohler, M.; Curtis, G. P.; Kent, D. B.; Davis, J. A. Experimental investigation and modeling of uranium(VI) transport under variable chemical conditions. *Water Resour. Res.* **1996**, *32*, 3539–3551.

(42) Stubbs, J. E.; Veblen, L. A.; Elbert, D. C.; Zachara, J. M.; Davis, J. A.; Veblen, D. R. Newly recognized hosts for uranium in the Hanford Site vadose zone. *Geochim. Cosmochim. Acta* **2009**, *73*, 1563–1576.

(43) Wang, Z.; Zachara, J. M.; Boily, J.; Xia, Y.; Resch., T.; Moore, D. A.; Liu, C. Determining individual mineral contributions to U(VI) adsorption in a contamination aquifer sediment: a fluorescence spectroscopy study. *Geochim. Cosmochim. Acta* **2011**, *75*, 2965–2979.

(44) Zhang, S.; Kent, D. B.; Elbert, D. C.; Shi, Z.; Davis, J. A.; Veblen, D. R. Mineralogy, morphology, and textural relationships in coasting on quartz grains in sediments in a quartz-sand aquifer. *J. Contam. Hydrol.* **2011**, *124*, 57–67.